Sensors and Materials, Vol. 26, No. 8 (2014) 581–589
MYU Tokyo

S & M 1024

Analytical and Experimental Studies on Human Body Communication between Wristwatch and Handheld Devices Using Muscle Homogenous Phantom at 10 MHz

Dairoku Muramatsu*, Fukuro Koshiji[1], Kohji Koshiji[2] and Ken Sasaki

Department of Human and Engineered Environmental Studies, Graduate School of Frontier Science, The University of Tokyo, 5-1-5 Kashiwano-ha, Kashiwa-shi, Chiba 277-8563 Japan
[1]Program in Electrical Engineering, Graduate School of Engineering, Kokushikan University, 4-28-1 Setagaya, Setagaya-ku, Tokyo 154-8515 Japan
[2]Department of Electrical Engineering, Graduate School of Science and Technology, Tokyo University of Science, 2641 Yamazaki, Noda-shi, Chiba 278-8510 Japan

(Received April 7, 2014; accepted August 6, 2014)

Key words: human body communication, wearable device, sensor network, electrode, electromagnetic field analysis, phantom

In human body communication, it is important to investigate the input impedance characteristics of electrodes and transmission characteristics between transceivers for improving the qualities of communication and reducing power consumption. In this work, we studied the input impedance characteristics and transmission characteristics between a wristwatch device and a handheld device using both a three-dimensional electromagnetic field simulation and experiment at 10 MHz. The input impedance and transmission characteristics obtained from the simulation using a muscle homogenous model and those obtained from the measurement using a muscle-tissue-equivalent phantom showed good consistency. The calculated electric field around a human arm decreased as it moved away from the surface of the arm. This distribution of the electric field showed the advantages of human body communication, which are confidential communication and electromagnetic compatibility (EMC). Moreover, power consumption at the feeding point of the system was calculated from the transmission characteristics obtained from the simulation. This result indicated that human body communication achieves low-power consumption.

*Corresponding author: e-mail: muramatsu@ems.k.u-tokyo.ac.jp

1. Introduction

High-density integration technology in recent years has provided wearable devices that are small in size and light in weight. As a result, people are expected to use multiple wearable devices in their daily life. One of the primary application fields for wearable devices is medical and welfare services, because multiple wearable devices are suitable for sensors detecting vital signals. The wearable sensor network for healthcare as shown in Fig. 1 is a prospective application of wearable sensors and devices.[1] In this system, vital signals collected by wearable sensors are transmitted to a smartphone by using a network in close proximity to a person's body, called a body area network (BAN).[2,3] The smartphone monitors the health condition of the user by an application. For further analysis, these data are transmitted to a medical server using existing infrastructure such as wireless local area network (WLAN). As a promising wireless communication method for BAN, human body communication that utilizes a part of the human body as a transmission medium has drawn much attention.[4] Human body communication has a high affinity with wearable devices attached to the human body because this technique mainly uses the human body and the space around the body for signal transmission. For the transmission mechanism, power consumption is small, and the radiated electric field is low. In the human body communication system, a radio frequency signal is excited in the human body through wearable electrodes (antennas). Therefore, it is important to clarify the input impedance and the transmission characteristics of the electrodes worn on the body for improving the transmission efficiency of devices. Electromagnetic field simulation is one of the useful solutions for clarifying the characteristics of the human body communication system in the development phase.[5]

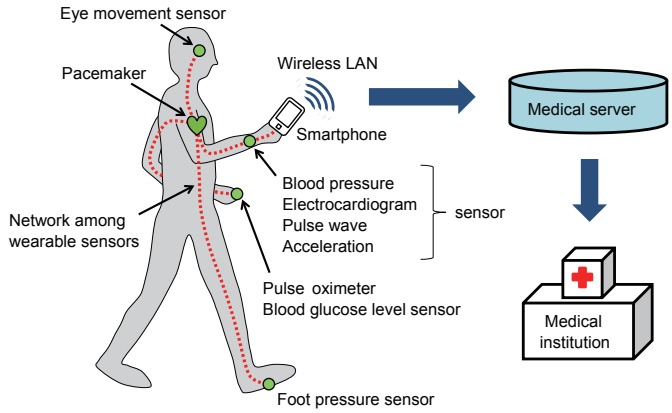

Fig. 1. (Color online) Wearable sensor network for health care.

In this work, we studied the input impedance characteristics, electric field around the human arm and transmission characteristics between a wristwatch device and a handheld device to clarify a mechanism of human body communication and to design a low-power communication system. First, the electric field around the human arm was calculated by a three-dimensional electromagnetic field simulation using a muscle homogenous arm model. The generated electric field around the human arm exponentially decreases as it moves away from the surface of the arm model. Second, for supporting the results obtained from the simulation, the input impedance and transmission characteristics were measured using prototype transceiver electrodes and a muscle-tissue-equivalent phantom. These analyzed and measured values showed good consistency. Moreover, power consumption at the feeding point of the system was calculated from the transmission characteristics obtained from the simulation. This result indicated that human body communication achieves low-power dissipation.

2. Materials and Methods

2.1 *Communication system*

In this research, we assumed communication between a wristwatch device (transmitter) installed on the front arm, including the wrist, and a handheld device such as a smartphone (receiver) in the hand. Figure 2 shows the proposed human body communication system. Electrodes (antennas) of these devices are assumed to be attached directly to the skin. The carrier frequency of the transmission was assumed to be 10 MHz because previous studies showed that the transmission efficiency peaks at approximately 10 MHz[6] and because we assumed the use of the industry-science-medical (ISM) band (13.56 MHz).[7] The output impedance of a large-scale integration (LSI) and measurement system of radio frequency is generally 50 Ω; therefore, we assumed a 50 Ω system.

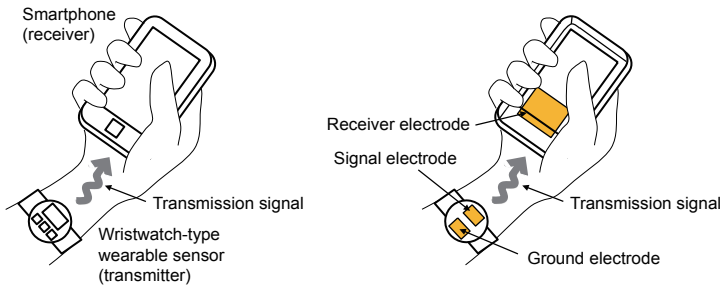

Fig. 2. (Color online) Human body communication system. (a) System image. (b) Electrode alignment.

2.2 *Analytical method*

Figure 3 shows a three-dimensional electromagnetic field analysis model of the system using the finite-difference time-domain (FDTD) method (Remcom, XFdtd). The human arm was modeled as a circular cylinder of radius r = 30 mm. The surface of the human arm model in contact with the transmitter and receiver electrodes is sliced off at 10% of the human arm diameter to make a plane surface for the contact (*e.g.*, if r = 30 mm, the human arm model is sliced off at 6 mm from the model surface; the width of the plane to the contact electrodes w is 36 mm). The human arm model length L_{arm} was 700 mm in consideration of the average human body size for a Japanese adult male.[8] From a previous study, the presence of the body is known to have little effect on the analysis results.[9] For this reason, we excluded the body from the analysis model. For the analysis, the human arm model had electrical characteristics of relative permittivity ε_r = 170 and electrical conductivity σ = 0.62 S/m; these are the values of muscle tissues at 10 MHz.[10] Figure 4 shows the structures of the transmitter and receiver model. The transmitter was located at the center of the arm model and constructed from a circuit board, a signal electrode, a ground electrode, wires, and an excitation point with an output impedance of 50 Ω. The receiver model was constructed from an upper electrode, a lower electrode, and a 50 Ω input load. All the materials for the transmitter and receiver models consisted of a perfect electric conductor (PEC). The dimensions of the transmitter and receiver electrode were decided assuming the size of a wristwatch-type wearable device and the size of a smartphone size device (transmitter: a_1 = 8.8, b_1 = 24, d = 6.4, L_1 = 24, L_2 = 24, h_1 = 10 mm, receiver: a_2 = 13, b_2 = 13, L_3 = 120, L_4 = 60, h_2 = 10 mm).[11,12] The computing space of FDTD simulation (260 × 260 × 900 mm^3) was represented by nonuniform grids. The sizes of these grids gradually increase as they move away from the vicinity of the transceiver electrodes. The grid size was

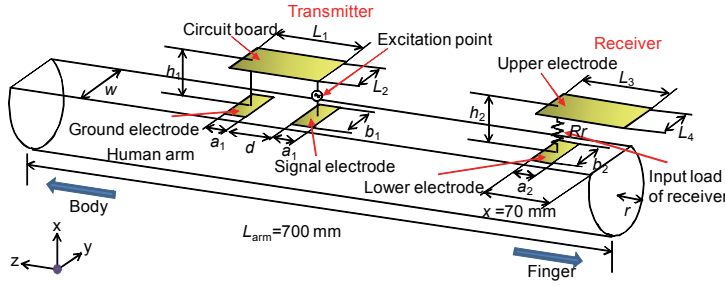

Fig. 3. (Color online) Muscle homogenous arm model for FDTD simulaton.

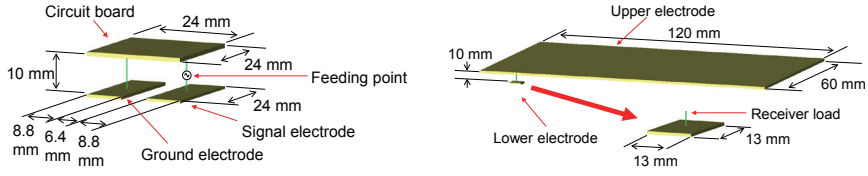

(a) (b)

Fig. 4. (Color online) Transceiver electrode model for electromagnetic field simulation. (a) Transmitter and (b) receiver.

1 mm around the transceiver electrodes and 5 mm at the edge of the computing space. A perfectly matched layer (PML) was used as an absorbing boundary. The number of layers was 7. A broadband pulse or a sinusoidal wave was fed at the feeding point, which is between the signal electrode and the circuit board. The time step of calculation was set to 1.60 ps.

2.3 *Experimental method*

In this section, we show the measurement system of the input impedance Z_{in} of the prototype transmitter and the transmission characteristics S_{21} between the prototype transmitter and receiver. The input impedance Z_{in} and transmission characteristics S_{21} were measured using a muscle-tissue-equivalent phantom (ε_r = 28, σ = 0.62 S/m at 10 MHz) as a human arm. From a previous study, if the conductivity of a phantom is consistent with human muscle, the difference in permittivity is known to have little effect on electric fields derived by the transmitter.[5] We also have already calculated the input impedance characteristics and transmission characteristics obtained from the different muscle models (ε_r = 170 or 28) by FDTD simulation. The differences in these characteristics between two models were sufficiently small. The designs of the prototype transmitter and receiver are shown in Fig. 5. The electrodes and circuit board of the transmitter and receiver consist of a copper plate, with styrene foam inserted as a supporter. The input impedance Z_{in} was measured using only one port of a vector network analyzer (VNA, Agilent, N5230A). Figure 6 shows the measurement system using a VNA, and Fig. 7 shows the measurement appearance. The measurement locations of the input impedance were 250, 300, and 350 mm from the tip of the human arm phantom.

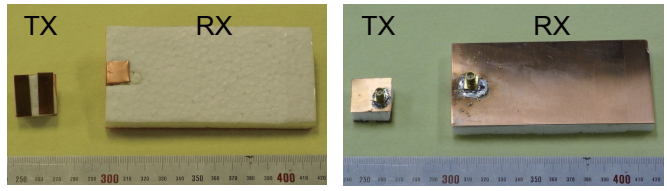

Fig. 5. (Color online) Prototype transmitter (TX) and receiver (RX).

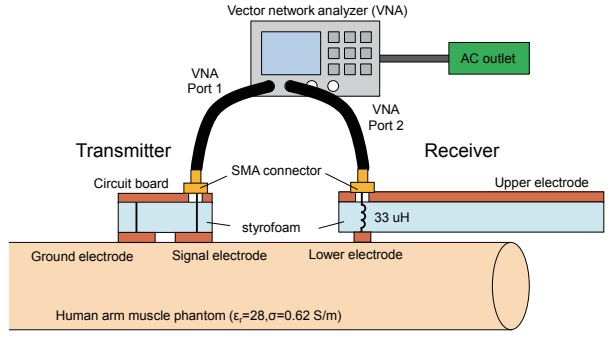

Fig. 6. (Color online) Measurement system comprised of vector network analyzer.

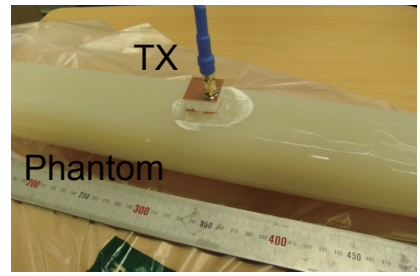

Fig. 7. (Color online) Measurement condition of input impedance characteristics of transmitter electrode.

S_{21} was measured using two ports of VNA with the measurement system shown in Fig. 6. Moreover, S_{21} was also measured using a signal generator (SG, Agilent, 83620A) and spectrum analyzer (SA, Agilent, E4407B) to consider the effect of the connection between the transmitter and receiver grounds. Figure 8 shows the system of the measurement using SG and SA, and Fig. 9 shows the appearance of measurement. SG was driven by a battery to avoid connecting grounds of SG and SA through the commercial power supply. The prototype transmitter and receiver were fixed by bands to be attached firmly to the phantom.

3. Results and Discussion

3.1 *Analytical results and discussion*

The input impedance characteristics Z_{in} of the electrodes were calculated by electromagnetic field simulation using the FDTD method. The input impedance was calculated as $Z_{in} = 50.2 - j6.6\ \Omega$ in the transmitter and $Z_{in}' = 49.2 - j2047\ \Omega$ in the receiver. For cancelling reactance components of the Z_{in} and Z_{in}' to reduce the reflection of the high-frequency signal, we inserted a 0.1 mH inductance to the feeding point of the transmitter and a 33 mH inductance to the load of the receiver. Under this condition, in the feeding point, the voltage standing wave ratio (VSWR) was calculated as 1.004, which fulfilled the criteria of VSWR ≤ 2 for good antennas. The transmission characteristic between the transmitter and receiver was calculated as $S_{21} = -44.2$ dB.

Figure 10 shows the electric field distributions around and inside the human arm at 10 MHz in the *zx* plane, including the feeding point of the transmitter. The dotted line shows the circumference of the arm model. This electric field distribution shows that the electric field 10 cm away from the arm surface is 10–20 dB lower than that at 5 cm away. Owing to this exponential decrease in the electric field, the signal propagates along the body without interference to other equipment. This is a good feature from the standpoint of confidential communication and electromagnetic compatibility (EMC).

3.2 *Experimental results and discussion*

We measured the input impedance Z_{in} of the prototype transmitter and the transmission characteristics S_{21} between the prototype transmitter and receiver using

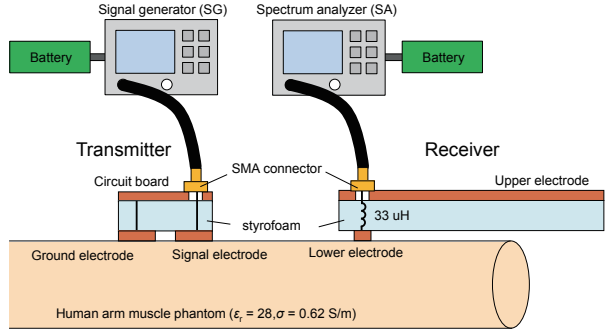

Fig. 8. (Color online) Measurement system comprised of signal generator and spectrum analyzer.

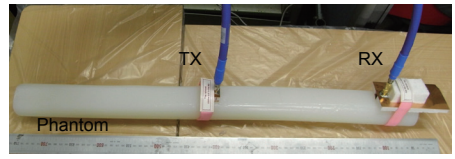

Fig. 9. (Color online) Measurement condition of transmission characteristics between transceiver electrodes.

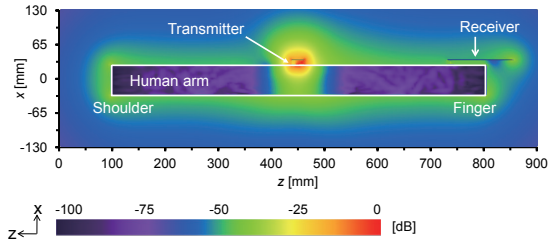

Fig. 10. (Color online) Electric field distribution around and inside the human arm.

a biological-tissue-equivalent phantom (ε_r = 28, σ = 0.62 S/m at 10 MHz). The input impedance Z_{in} was measured using the system shown in Fig. 6. The measurement locations of the input impedance were 250, 300, and 350 mm from the tip of the human arm phantom. As shown in Fig. 11, the measured values and analyzed values showed good consistency at each location. The transmission characteristics S_{21} were measured using the measurement system shown in Figs. 6 and 8. As shown in Table 1, the transmission characteristics were measured as S_{21} = −47.0 dB by using VNA, and S_{21} = −47.5 dB by using SG and SA. These measured values were close to the analyzed value of S_{21} = −44.2 dB. These results support the results of the FDTD simulation demonstrated in § 3.1.

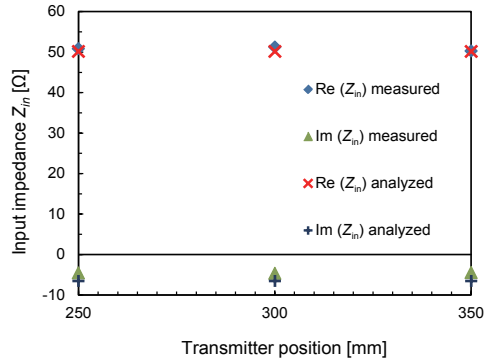

Fig. 11. (Color online) Input impedance characteristics of transmitter electrode as a function of transmitter position.

Table 1
Transmission characteristics between transceiver electrodes.

Analyzed (FDTD)	Measured (VNA)	Measured (SG+SA)
−44.2 dB	−47.0 dB	−47.5 dB

For reference, if the receiver needs at least −80 dBm received power for communication, when S_{21} is −44.2 dB (analytic value), 30 mV should be input at the excitation point of the transmitter. In this instance, the power consumption at the feeding point is 4.5 μW. For example, the transmitted power at the antenna of Bluetooth class 3 is 1 mW. The 4.5 μW power consumption of the transmitter electrode (antenna) is extremely small compared with that of Bluetooth class 3. This calculation of the power consumption indicates that human body communication achieves low-power dissipation.

4. Conclusions

In this work, we studied the input impedance characteristics and transmission characteristics between a wristwatch device and a handheld device both analytically and experimentally. The analytical results obtained from the FDTD simulation showed that the intensity of the electric field exponentially decreases as it moves away from the surface of the arm model. This is a good feature from the standpoint of confidential communication and EMC. Moreover, the experimental results obtained from the measurement with the prototype transceiver and phantom agreed well with that obtained from the FDTD simulation. These experimental results support the results of the electromagnetic field simulation in the calculation of human body communication characteristics. These analytical and experimental studies also indicated that human body communication achieves low-power dissipation.

Acknowledgements

A part of this research was carried out through a Grant-in-Aid for JSPS Fellows (25-5924).

References

1 T. Ozaki, M. Omi, C. Sugimoto, K. Shiba, K. Naemura, H. Hosaka, K. Itao and K. Sasaki: Micromechatronics **47** (2003) 12.
2 H.-B. Li, K. Takizawa and R. Kohno: Proc. 1st European Wireless Technology Conf., 2008, p. 1.
3 IEEE Standard for Local and Metropolitan Area Networks Part 15.6: Wireless Body Area Networks, IEEE Computer Society (2012).
4 T. G. Zimmerman: IBM Syst. J. **35** (1996) 609.
5 K. Fujii, K. Ito and S. Tajima: IEICE Trans. Commun. **J87-B** (2004) 1383.
6 K. Hachisuka, T. Takeda, Y. Terauchi, K. Sasaki, H. Hosaka and K. Itao: IIP/ISPS Joint MIPE '03 (2003) pp. 139–140.
7 International Telecommunication Union, http://www.itu.int/en/pages/default.aspx (accessed on March 2014).
8 Research Institute of Human Engineering for Quality Life: Human body dimensions data for ergonomic design (1996).
9 F. Koshiji and K. Sasaki: J. JIEP **12** (2009) 221.
10 R. Gabriel, W. Lau and C Gabriel: Phys. Med. Biol. **41** (1996) 2251.
11 D. Muramatsu, T. Yamamoto, F. Koshiji and K. Koshiji: J. JSAEM **19** (2011) 354.
12 D. Muramatsu, T. Yamamoto, F. Koshiji, K. Koshiji and K. Sasaki: J. Life Support Eng. **24** (2012) 70.